



## Philosophical Magazine

Publication details, including instructions for authors and subscription information:

<http://www.tandfonline.com/loi/tphm20>

### Thermal characterization of nanocrystalline porous CePO<sub>4</sub> ceramics

Sajan D. George<sup>a,c</sup>, Rajesh Kombar<sup>b</sup>, K.G.K. Warriar<sup>b</sup>, P. Radhakrishnan<sup>c</sup>, V.P.N. Nampoore<sup>c</sup> & C.P.G. Vallabhan<sup>c</sup>

<sup>a</sup> Center of Smart Interfaces, TU Darmstadt, Petersenstrasse 32, 64287, Darmstadt, Germany

<sup>b</sup> Ceramic Technology Division, Regional Research Laboratory, CSIR, Thiruvananthapuram 695019, India

<sup>c</sup> International School of Photonics, Cochin University of Science and Technology, Cochin 682022, India

Available online: 03 Feb 2010

To cite this article: Sajan D. George, Rajesh Kombar, K.G.K. Warriar, P. Radhakrishnan, V.P.N. Nampoore & C.P.G. Vallabhan (2010): Thermal characterization of nanocrystalline porous CePO<sub>4</sub> ceramics, Philosophical Magazine, 90:6, 717-729

To link to this article: <http://dx.doi.org/10.1080/14786430903246312>

PLEASE SCROLL DOWN FOR ARTICLE

Full terms and conditions of use: <http://www.tandfonline.com/page/terms-and-conditions>

This article may be used for research, teaching, and private study purposes. Any substantial or systematic reproduction, redistribution, reselling, loan, sub-licensing, systematic supply, or distribution in any form to anyone is expressly forbidden.

The publisher does not give any warranty express or implied or make any representation that the contents will be complete or accurate or up to date. The accuracy of any instructions, formulae, and drug doses should be independently verified with primary sources. The publisher shall not be liable for any loss, actions, claims, proceedings, demand, or costs or damages whatsoever or howsoever caused arising directly or indirectly in connection with or arising out of the use of this material.

## Thermal characterization of nanocrystalline porous CePO<sub>4</sub> ceramics

Sajan D. George<sup>ac\*</sup>, Rajesh Komban<sup>b</sup>, K.G.K. Warriar<sup>b</sup>,  
P. Radhakrishnan<sup>c</sup>, V.P.N. Nampoore<sup>c</sup> and C.P.G. Vallabhan<sup>c</sup>

<sup>a</sup>Center of Smart Interfaces, TU Darmstadt, Petersenstrasse 32, 64287, Darmstadt, Germany; <sup>b</sup>Ceramic Technology Division, Regional Research Laboratory, CSIR, Thiruvananthapuram 695019, India; <sup>c</sup>International School of Photonics, Cochin University of Science and Technology, Cochin 682022, India

(Received 28 February 2009; final version received 9 August 2009)

A laser-induced photoacoustic technique was employed to investigate thermal transport through nanocrystalline CePO<sub>4</sub> samples prepared via the sol–gel route. Evaluation of thermal diffusivity was carried out using the one-dimensional model of Rosencwaig and Gersho for the reflection configuration of the photoacoustic method. Structural analyses of samples revealed that they are nanoporous in nature, possessing micron-sized grains. Analysis of results shows that thermal diffusivity value varies with sintering temperature. Results are explained in terms of the variation in porosity with sintering temperature and the effects of various scattering mechanisms on the propagation of phonons through the nanoporous ceramic matrix. Further analyses confirm that apart from porosity, grain boundary resistance and interface thermal resistance influence the effective value of thermal diffusivity of the samples under investigation.

**Keywords:** photoacoustics; nanocrystalline ceramics; sol–gel method; thermal diffusivity

### 1. Introduction

Research towards a better understanding of the physical properties of heterogeneous solids has both scientific and technological importance [1,2]. In recent years, rare earth phosphates have become increasingly important for several applications, which include ceramic materials, catalysts, photoluminescence materials, dielectric substrates, metal surface treatment agents, optical materials, etc. [3–6]. Other potential applications of these materials include host matrices for immobilization of actinide radio-nuclear wastes, solid protonic conductors and weak fiber matrix interfaces in ceramic–ceramic composites or thermal protection coatings [7–10]. Of late, synthesis of nanocrystalline rare earth phosphates has been attempted via various methods, such as the sol–gel method, the surfactant-directed hydrothermal approach, etc. [11,12]. Cerium phosphate is an important class of rare earth phosphate ceramic, which has immense use in high temperature applications due to

---

\*Corresponding author. Email: george@csi.tu-darmstadt.de

its high melting point. Apart from its potential as a storage material for nuclear waste and poison to automobile catalyst, recently it has been used as proton conduction membrane in hydrogen fuel cells [13]. However, the chemical and physical properties of these ceramics depend greatly on the processing technique and conditions. Although various aspects of nanocrystalline ceramics have already been investigated, measurement of thermal parameters of sol-gel prepared nanocrystalline  $\text{CePO}_4$  has not been investigated in detail.

Since the Rosenzweig-Gersho (R-G) theory was proposed for the photoacoustic effect in solids [14], photothermal methods have been used to determine several material properties in different states of matter where conventional spectroscopic methods fail [15–17]. Amongst various photothermal techniques, the photoacoustic (PA) method has become more popular due to its simplistic approach. The PA effect directly looks into the heat generated in the sample due to non-radiative de-excitation processes following an optical excitation of the sample with modulated or pulsed light [17]. Data on the thermal properties are vital for any material employed in devices with thermal dissipation. Thermal diffusivity is a unique and important thermophysical parameter, which measures the rate of diffusion of heat in a material. Physically, the inverse of thermal diffusivity is a measure of the time required to establish thermal equilibrium in a system in which transient temperature change has occurred [18–21]. As a result, thermal diffusivity is directly related to microstructure and thereby the processing conditions of ceramics.

In our previous work, we reported the thermal characterization of porous  $\text{LaPO}_4$  ceramics using a photothermal technique [21]. In this paper, work is focused on the evaluation of thermal diffusivity of nanocrystalline  $\text{CePO}_4$  prepared via the sol-gel process and the influence of sintering temperature on thermal diffusivity. Sintering is the process whereby interparticle pores in a granular material are eliminated by atomic diffusion driven by capillary forces. The process of sintering can profoundly influence the porosity of nanocrystalline ceramics and thereby the heat transport through materials. Porous ceramics are receiving considerable attention due to their applications in variety of areas, such as thermal and noise isolation, liquid and gas infiltration, catalyst products, electronics and biomedical applications [22–24]. Hence, a detailed investigation of the influence of sintering on porosity and hence on thermal diffusivity is of great relevance, especially from the device fabrication point of view.

## 2. Sample preparation

Cerium nitrate, 99.9% pure (M/s Indian Rare Earths Ltd, India) and orthophosphoric acid (AR grade, 88%, Qualigens Fine Chemicals, India) were used as starting materials. A 0.03 M (9.239 g) solution of  $\text{Ce}(\text{NO}_3)_3 \cdot 6\text{H}_2\text{O}$  was prepared in de-ionized water. Orthophosphoric acid solution (2.084 g, 1.191 ml) was added drop-wise to the cerium nitrate solution under constant stirring. An off-white precipitate of cerium phosphate was obtained. The precipitate was filtered and washed free of nitrates and phosphates, and was further re-dispersed in de-ionized water. Electrostatic stabilization was achieved by the addition of 20% nitric acid, with the pH maintained in

the range 1.8–2. The suspension was stirred continuously for about 4 h. The colloidal sol thus obtained was further subjected to ultrasonication for 15 min to obtain stable cerium phosphate precursor sol. Gelation of the sol was carried out by exposing it to ammonia atmosphere for a period of two days. Cerium phosphate gel thus obtained was dried at 80°C and calcined at 400°C at a rate of 10°C min<sup>-1</sup> under air atmosphere to yield cerium phosphate gel powder. The relative density of cerium phosphate sintered at different temperatures was measured using the Archimedes displacement method. The porosity,  $p$ , of specimens having relative density  $x$  was evaluated knowing that  $p = 1 - x$  [25] (see Table 1).

Phase identification was carried out by X-ray diffraction (XRD, Philips PW 1710) on the calcined powders using Cu-K $\alpha$  radiation (Figure 1). The gel calcined at 400°C exhibits a transformation from rhabdophane to the hexagonal form. The major hexagonal cerium phosphate phase was identified with JCPDS file no 4-362 and the presence of rhabdophane (JCPDS file no 35-0614) in the XRD pattern also shows the incomplete transformation of hexagonal phase. The sample calcined at 800°C exhibits broad peaks of monazite-type monoclinic cerium phosphate (JCPDS file no 32-0199), which became sharp above this temperature.

The crystallite size, calculated using the X-ray line broadening method using the Scherrer equation,  $t = \frac{0.9\lambda}{\beta \cos \theta}$ , where  $t$  is the crystallite size,  $\lambda$  is wavelength of radiation (1.54 Å for Cu-K $\alpha$  radiation),  $\beta$  is the corrected peak width at half maximum intensity, and  $\theta$  is the angle of diffraction at the peak position, is shown in Figure 2. The crystallite size ranges from 10 to 40 nm and it increases with sintering temperature.

The calcined powder was compacted at a pressure of 200 MPa to pellets of size 11 mm and thickness around 500  $\mu$ m and sintered in the range 800 to 1700°C, at a heating rate of 10°C min<sup>-1</sup> and soaked for 3 h. BET surface area and pore size distribution of the gel after calcination at 400 and 800°C were measured by nitrogen adsorption after degassing the powders at 200°C for 4 h using Micromeritics Gemini 2375 V5.01 surface area analyzer. The pore size distribution was obtained by the Barrett–Joiner–Halenda (BJH) method from the desorption curve of the isotherm using the Micromeritics Star Driver version 2.03 software.

Table 1. Thermal diffusivity of CePO<sub>4</sub> ceramics.

Sintering temperature (°C)	Porosity (%)	Measured thermal diffusivity (cm <sup>2</sup> s <sup>-1</sup> )	Calculated thermal diffusivity (cm <sup>2</sup> s <sup>-1</sup> )
800	46	0.140 ± 0.004	0.142
900	42	0.250 ± 0.007	0.252
1000	38	0.342 ± 0.006	0.344
1100	27.5	0.534 ± 0.008	0.540
1200	4.3	0.820 ± 0.004	0.822
1300	0.5	0.846 ± 0.005	0.855
1400	1	0.846 ± 0.007	0.851
1500	2.5	0.840 ± 0.004	0.847
1600	6.5	0.790 ± 0.008	0.801
1700	8	0.786 ± 0.006	0.793

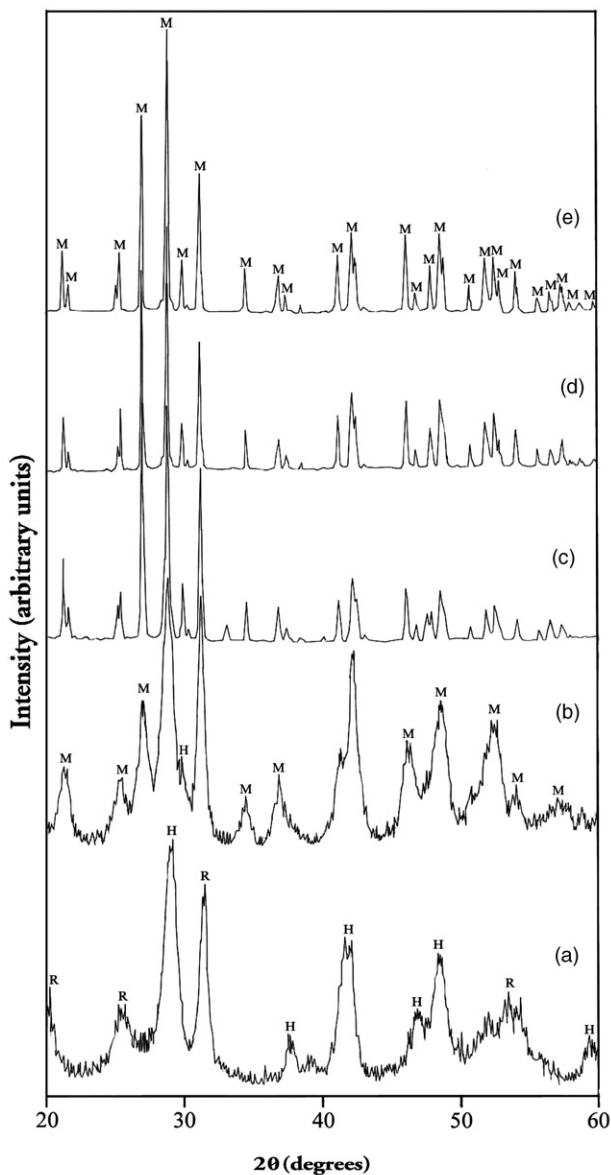


Figure 1. X-ray diffraction patterns of cerium phosphate precursor gel heated at different temperatures: (a) 400°C; (b) 800°C; (c) 1000°C; (d) 1300°C; (e) 1700°C. M – monazite, H – hexagonal, R – rhabdophane.

### 3. Experimental

A schematic view of the experimental setup is shown in Figure 3. Optical radiation from an argon ion laser at 488 nm (Liconix 5300) was used as the source of excitation, and it was intensity modulated using a mechanical chopper (Stanford Research Systems SR 540) before it reached the sample surface. Detection of

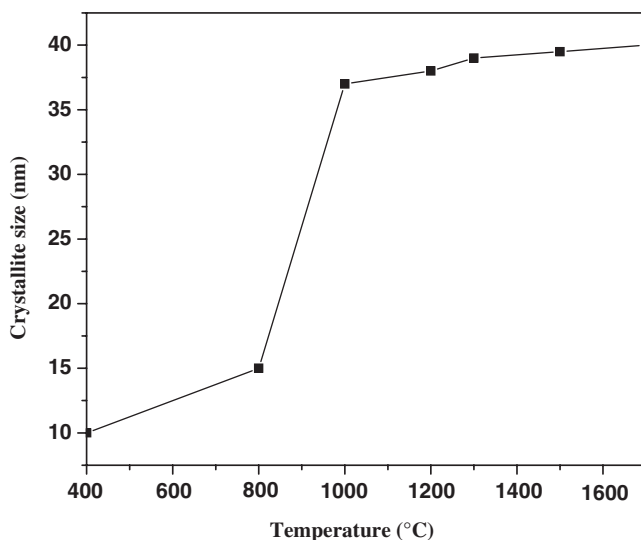


Figure 2. Plot of crystallite size versus temperature.

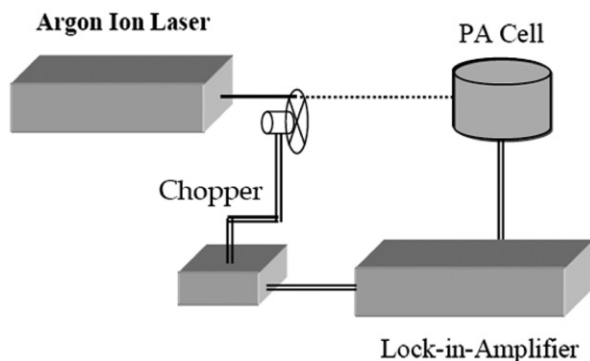


Figure 3. Schematic view of experimental setup.

pressure fluctuations (photoacoustic signal) in the cell cavity was done using a sensitive microphone (Knowles BT 1754). The amplitude of the photoacoustic signal was measured using a dual phase lock-in amplifier (Stanford Research Systems SR 830). The laser power used for the present studies was 50 mW with a stability of  $\pm 0.5\%$ . A homemade PA cell was employed for the present studies. The cell was made using an acrylic polymer (Perspex) and the volume of the cell was designed such that PA amplitude was maximum and large enough to avoid thermoviscous damping of acoustic signals at the cell wall. The PA cell was fabricated on the cell material with 5 cm diameter and 1 cm thickness by drilling bore of diameter 3 mm, along its thickness direction, through its center. Another fine bore of diameter 1.5 mm pierced at the middle of the main chamber and directed perpendicular to it served as the acoustic coupler between the main chamber and the microphone. At a

distance of 8 mm from the main chamber the microphone was fixed to the orifice of side tube. In this case, the thermal diffusion length in air is smaller than acoustic cell diameter and thus one-dimensional model of R-G theory can be used. More details about the setup can be found elsewhere [26].

#### 4. Theoretical background

According to the one-dimensional model proposed by Rosencwaig and Gersho [14], the pressure variation,  $\delta P$ , at the front surface of an optically thick ( $l \gg 1/\mu$ , where  $\mu$  is the optical absorption length) sample irradiated with a chopped beam of monochromatic radiation depends on the thermal diffusivity,  $\alpha_s$ , of the sample. The theoretical expression for  $\delta P$  may be written as

$$\delta P = XY. \quad (1)$$

In the above expression,

$$X = \left[ 1 + g \frac{h^+ + h^-}{h^+ - h^-} \right] \left[ g + \frac{h^+ + h^-}{h^+ - h^-} \right] \frac{1}{x_s^2 l_s^2}, \quad (2)$$

where

$$h^+ = \exp(\sigma_s l_s),$$

$$h^- = \exp(-\sigma_s l_s)$$

and

$$\sigma_s = (1 - j) \left( \frac{\pi f}{\alpha_s} \right)^{\frac{1}{2}}, \quad (3)$$

where

$$j = \sqrt{-1}. \quad (4)$$

In Equation (2),

$$g = \frac{e_b}{e_s} = \left( \frac{K_b}{K_s} \right) \left( \frac{\alpha_s}{\alpha_b} \right)^{\frac{1}{2}} \quad (5)$$

is the ratio between effusivities of backing material ( $e_b$ ) and the sample ( $e_s$ ). In Equation (1),

$$Y = \frac{P_o \gamma W_a l_s^2}{2 l_g T_o K_s} \left( \frac{\alpha_s}{\alpha_b} \right)^{\frac{1}{2}}, \quad (6)$$

where  $l$  and  $K$  indicate the length and thermal conductivity of the corresponding part of the geometry shown in Figure 4 and the subscripts  $g$ ,  $s$  and  $b$  refer to gas, sample and backing respectively.  $P_o(T_o)$  is the ambient pressure (temperature);  $\gamma$  is the specific heat ratio of air.  $W_a$  is the absorbed power of optical radiation.

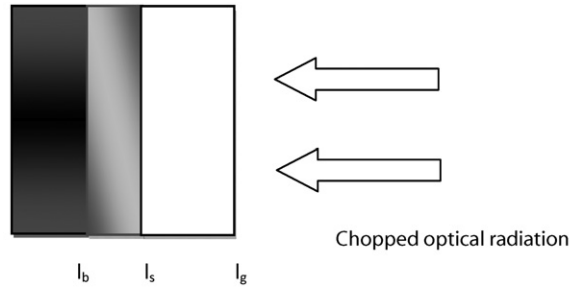


Figure 4. Geometry of photoacoustic configuration.

The effusivity of the gas can be neglected in comparison to the effusivity of sample, since their ratio is always less than 1%. The term  $X$  depends on the modulation frequency through the product  $\sigma_s l_s$ , which can be written as

$$\sigma_s l_s = (1 - j) \left( \frac{\pi f}{f_c} \right)^{\frac{1}{2}}, \quad (7)$$

where the characteristic frequency  $f_c$  is given by

$$f_c = \frac{\alpha_s}{l_s^2}. \quad (8)$$

When thermal diffusion length,  $d = \left( \frac{\alpha}{\pi f} \right)^{\frac{1}{2}}$ , is greater than the sample thickness, thermal properties of the backing material determine the PA signal. But in the thermally thick regime, the PA signal is independent of the thermal properties of backing material. For a given sample thickness, there is a transition from thermally thin regime to thermally thick regime with variation in chopping frequency. Such a transition is exhibited in the amplitude spectrum of the PA signal, which is evinced by the change in slope and by knowing the transition frequency and thickness of the specimen; thermal diffusivity can be evaluated using Equation (8).

## 5. Results and discussions

Initially, the experimental setup used for the investigation was calibrated by evaluating the thermal diffusivity of GaAs and Al. The measured values of thermal diffusivity ( $0.260 \pm 0.03 \text{ cm}^2 \text{ s}^{-1}$  and  $0.978 \pm 0.03 \text{ cm}^2 \text{ s}^{-1}$ , respectively) agree well with earlier reported values [18,27]. Figure 5 shows the amplitude spectrum of the PA signal for the sample sintered at  $800^\circ\text{C}$ . All other samples show similar behavior (not shown here).

The thermal diffusivity values of cerium phosphate sintered at different temperatures were evaluated from the amplitude spectrum of PA signal and are given in Table 1. From the values, it is obvious that sintering temperature affects porosity of the specimen and thereby influences the thermal diffusivity value.



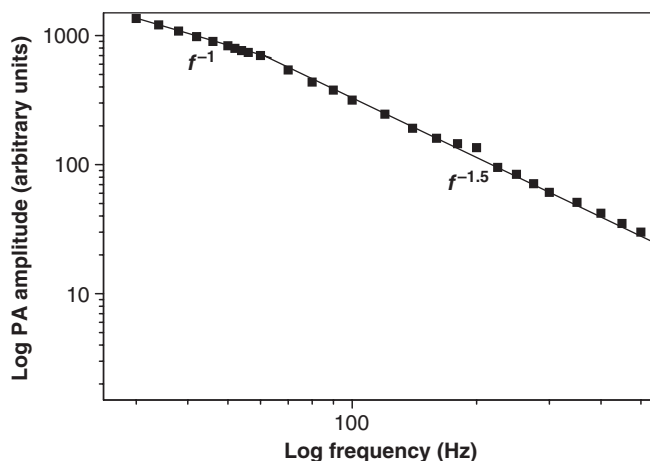


Figure 5. Log–log plot of PA amplitude of  $\text{CePO}_4$  sintered at  $800^\circ\text{C}$ .

Thermal transport properties of polycrystalline dielectric materials such as those investigated here are directly influenced by materials composition, structure and arrangement of phases. In the case of heterogeneous materials such as ceramics, local variation in thermal parameters can occur because of the presence of different solid phases, pores, boundary resistance, etc., and thereby affect the propagation of thermal energy carriers [28–32]. The appearance of porosity amounts to a new phase in ceramic materials prepared through the gel route. In the case of porous ceramics, heat transport could be primarily due to two processes, phonon and radiative transport [33]. The former relates to the movement of atoms in the crystalline lattice, whereas the latter is due to electron transitions between energy levels in these atoms. If we neglect the relation between energy levels and spacing between the atoms, then both mechanisms can be considered independently. Such an assumption seems to be reasonable if the amplitude of atomic oscillations is considerably smaller than the lattice constant [22]. In general, the radiative contribution arises from photon emission caused by electron transport. However, in the case of dielectrics at room temperature, the density of electrons is negligibly small and thermal energy is carried mainly by phonons. The influence of pores on thermal conductivity value has already been investigated [31–33]. For cases in which the damping wavelength of thermal waves,  $L_{th} = 2\pi d$ , is greater than or of the order of typical grain size ( $L$ ), “thermal disturbance” is not affected by the heterogeneity of sample and the measurements then yield the “global thermal diffusivity” [34], which is the case for all samples in the present study. However, the pores in the lattice can act as scattering centers for phonons and hence affect the phonon mean free path and consequently their thermal diffusivity value. The pore size distribution and  $\text{N}_2$  adsorption characteristics of cerium phosphate gel after calcination at  $400^\circ\text{C}$  and  $800^\circ\text{C}$  are shown in Figures 6a and 6b, respectively. The presence of micropores ( $<20 \text{ \AA}$ ) with extended mesoporosity ( $20\text{--}500 \text{ \AA}$ ) is seen in calcined gels. On heating to  $800^\circ\text{C}$ , the volume of smaller pores up to around  $100 \text{ \AA}$  decreases considerably and a corresponding decrease in surface area from  $96$  to  $49 \text{ m}^2 \text{ g}^{-1}$  is observed when the gel is heated at

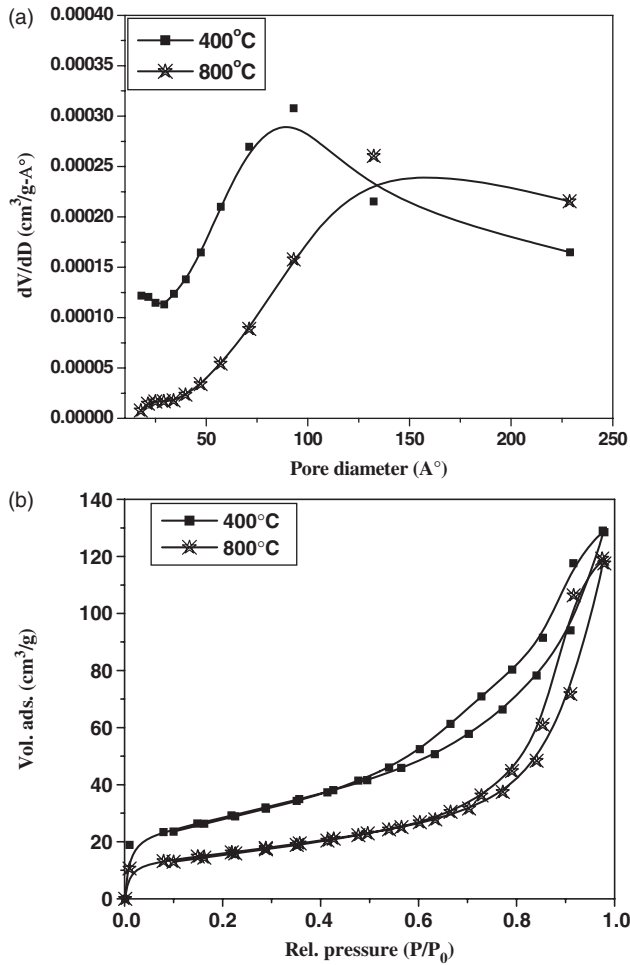


Figure 6. (a) Pore size distribution of cerium phosphate precursor gel after calcinations at 400 and 800°C. (b)  $\text{N}_2$  adsorption isotherm of cerium phosphate precursor gel after calcinations at 400 and 800°C.

400°C and 800°C, respectively. The BET isotherms with characteristic loop clearly indicate a type IV, i.e. mainly mesoporous textures, although at relatively low pressure ( $P/P_0$ ) it shows microporous character. Compared with the 800°C calcined sample, the volume of adsorption of  $\text{N}_2$  is much higher in the case of the 400°C calcined sample at all relative pressures. Generally, as the pore sizes are much smaller than the damping wavelength of thermal waves, the measured values in this study are the effective thermal parameters of specimen.

As reported previously [28–30], density variations and hence porosity variations caused by the sintering temperature of the samples under investigation can affect the thermal conductivity value. By considering porous ceramics as a two-phase network in which pores are randomly embedded in a solid matrix, the thermal diffusivity of the specimen is given by the expression,  $k_c(p) = \frac{K_c(p)}{\rho_0 C_0(1-p)}$ , where  $K_c(p)$  is the thermal

conductivity of the specimen having porosity  $p$ ;  $\rho_0$  and  $C_0$  are the density and specific heat capacity of the sample with zero porosity [35]. If the thermal conductivity of the porous material is modified by the same ratio as that of the ratio between actual density and maximum density, then thermal conductivity is given by Leob equation [36],  $K_c(p) = K_0(1 - p)$ . However, such a methodology to evaluate thermal conductivity yields thermal diffusivity value that is independent of porosity, which contradicts our experimental observation. All the studies done on samples prepared via sol-gel route show a dependence of thermal diffusivity value on porosity. A similar influence of porosity on heat transport of ceramics has already been investigated [37]. In order to incorporate the influence of porosity on the propagation of thermal waves and hence on the measured thermal diffusivity values, Sanchez-Lavega et al. [38] modified the Leob equation for thermal diffusivity as  $k_c(p) = k_0 \frac{(1-np)}{(1-p)}$ , where  $n$  is an empirical constant. From Table 1, it is clear that the measured thermal diffusivity values agree well with that calculated using modified Leob equation. Increase in density and a consequent decrease in porosity with sintering temperature results in a proportional reduction in scattering centers for phonons with sintering temperature, which consequently affects the phonon mean free path. The lattice thermal conductivity (thermal diffusivity) which is also proportional to phonon mean free path, thus varies in accordance with variations in porosity. Dependence of thermal diffusivity of all the samples under investigation on porosity indicates that the samples are below their percolation threshold. Percolation threshold is the limit above which a specific physical property (e.g. thermal diffusivity, hardness, stiffness etc.) is insensitive to further changes in relative density. Above percolation threshold, particle-particle contact is insufficient to fully transmit the physical forces [23].

The calculated value of empirical constant  $n (=1.98) > 1$  suggests that the effect of porosity on heat conduction in all the samples under study is not a mere density effect (air holes in the bulk specimen). A value of  $n=1$  suggests that thermal diffusivity value becomes equal to  $k_0$  and thus thermal diffusivity value is independent of porosity. A value of  $n < 1$  suggests that porous ceramics can exhibit higher thermal diffusivity value compared to samples with zero porosity, which contradicts our experimental observation as well as the scattering mechanisms in porous ceramics. Evaluation of thermal conductivity using the relation thus affects the propagation of phonons through the specimen, apart from porosity (or density). In the case of larger grain sized nanocrystals, the majority of heat is carried away by well defined quanta of propagating and polarized vibrational modes (i.e. phonons). Hence, the actual value of thermal parameters is determined by the mean free path of phonons between the scattering events. The mean free path of phonons is essentially determined by various scattering mechanisms in ceramics such as phonon-phonon scattering, phonon-electron scattering, phonon-grain boundary scattering, phonon-defect scattering, etc. [30]. In the case of samples investigated here, phonon-electron scattering can be neglected as the densities of free electrons are negligibly small. However, grain boundaries affect the propagation of phonons and hence their thermal diffusivity value. If the grain boundary has a significant thickness, phonons will be scattered a few times inside the grain boundary phase and the thermal conductivity of grain boundary phase plays a significant role in determining the effective thermal parameters. If the grain boundaries are thin enough, phonons may

scatter once at the grain boundary and then the phonon scattering sites in sample grains will control the effective thermal parameters of sintered samples [39]. SEM analysis of our samples sintered at 1300°C (Figure 7) and 1500°C (Figure 8) shows that grain size increases from 1  $\mu\text{m}$  to 2  $\mu\text{m}$  for samples sintered at 1300°C and 1500°C, respectively. As the sintering temperature increases, grain size increases

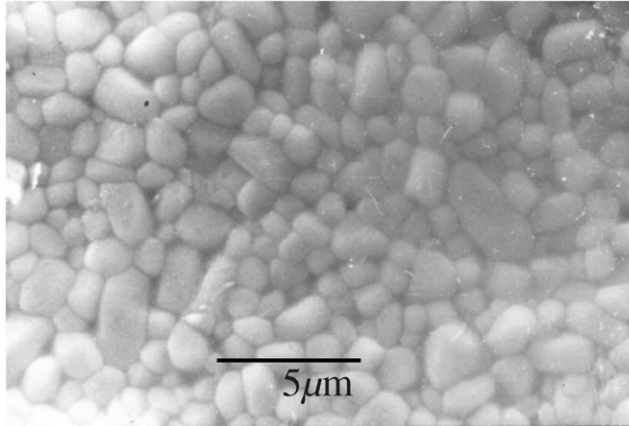


Figure 7. SEM of cerium phosphate sintered at 1300°C.

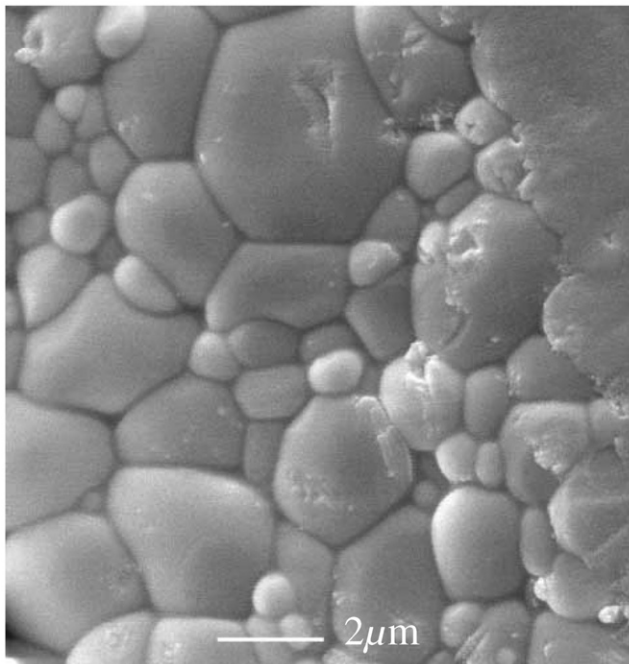


Figure 8. SEM of cerium phosphate sintered at 1500°C.

resulting in reduction in grain boundaries and a consequent increase in phonon mean free path and hence thermal diffusivity value.

A recent investigation shows that for dense samples, the phonon mean free path is smaller than the grain size at all processing temperatures [40]. Hence, in addition to porosity, the defects in grains also contribute to the variation in thermal diffusivity [41] and this explains the value of  $n > 1$ . An investigation on porous ceramic alumina shows that the solid area fraction (SAF) in the direction of heat flow also affects the measured thermal diffusivity value [23]. Enhancement in solid area fraction with increase in sintering temperature results in cohesive thermal transport with reduced scattering due to defects and interfaces. Thermal contact resistance ( $R_T$ ) at the interface is related to macroscopic thermal conductivity ( $K_c$ ) and to the grain conductivity ( $K$ ) through the relation  $\frac{L}{K_c} = \frac{L}{K} + R_T$ , where  $L$  is the grain size [42]. Increase in sintering temperature results in enhanced contribution from grain conductivity due to more ordered structure and reduction in interface thermal resistance.

## 6. Conclusions

In this article, we have reported measurements of the thermal diffusivity of  $\text{CePO}_4$  (prepared by the sol-gel process) using a laser-induced non-destructive photo-acoustic technique. The present study clearly shows that sintering temperature and consequent variation in porosity alters the scattering center concentration for phonons propagating through the lattice. From the analysis of results, it is evident that the transient thermophysical parameter, i.e. thermal diffusivity, varies substantially with sintering temperature. An empirical relation of thermal diffusivity on porosity shows that propagation of phonons and hence thermal diffusivity value is not merely affected by porosity, but by other factors such as grain boundary resistance and interface thermal resistance. The present investigation also shows that, by measuring thermophysical parameters, the simple and elegant PA technique can throw light on structural variations of ceramics caused by variations in processing conditions. Such tunability in thermal properties with processing conditions and evaluation of thermal diffusivity of these materials could find applications in the microelectronic and optoelectronic industry.

## References

- [1] J. Sun, *Int. J. Ceram. Tech.* 4 (2007) p.75.
- [2] Q. Huang, L. Gao, Y. Liu and J. Sun, *J. Mater. Chem.* 15 (2005) p.1995.
- [3] K. Popa, D. Sedmidubsky, O. Benes, C. Thiriet and R.J.M. Konings, *J. Chem. Therm.* 38 (2006) p.825.
- [4] H. Meyssamy, K. Riwozaki, A. Kronowski, S. Naused and M. Hasse, *Adv. Mater.* 11 (1999) p.840.
- [5] P.E.D. Morgan and D.B. Marshall, *J. Am. Ceram. Soc.* 78 (1995) p.1553.
- [6] Y. Hikichi and T. Nomura, *J. Am. Ceram. Soc.* 70 (1987) p.C-252.
- [7] L.A. Boatner, M.M. Abraham and B.C. Sales, *Inorg. Chim. Acta* 94 (1984) p.146.
- [8] T. Norby and N. Christiansen, *Solid State Ionics* 77 (1995) p.240.

- [9] Y. Hikichi and T. Ota, Phosphorus Res. Bull. 6 (1996) p.175.
- [10] Y. Hikichi and T. Ota, Mineral. J. 19 (1997) p.123.
- [11] S. Lucas, E. Champion, D. Bernache-Assollant and G. Leroy, J. Solid State Chem. 177 (2004) p.1312.
- [12] L. Karpowicha, S. Wilkeb, Rong Yuc, G. Harleya, J.A. Reimerb and L.C. De Jonghe, J. Solid State Chem. 180 (2007) p.840.
- [13] D. Bregiroux, S. Lucas, E. Champion, F. Audubert and D. Bernache-Assollant, J. Eur. Ceram. Soc. 26 (2006) p.279.
- [14] A. Rosencwaig and A. Gersho, J. Appl. Phys. 47 (1976) p.64.
- [15] A. Mandelis, S.B. Peralta and J. Thoen, J. Appl. Phys. 70 (1991) p.1761.
- [16] M. Chirtoc, I. Chirtoc, S. Pittois, C. Glorieux and J. Thoen, Rev. Sci. Instrum. 74 (2003) p.632.
- [17] B. Li and E. Welsch, Appl. Opt. 38 (1999) p.5241.
- [18] S.D. George, P. Radhakrishnan, V.P.N. Nampoouri and C.P.G. Vallabhan, Phys. Rev. B 68 (2003) p.163519.
- [19] S.D. George, S. Saravanan, M.R. Anantharaman, S. Venketachalam, P. Radhakrishnan, V.P.N. Nampoouri and C.P.G. Vallabhan, Phys. Rev. B 69 (2004) p.235201.
- [20] S.D. George, P. Radhakrishnan, V.P.N. Nampoouri and C.P.G. Vallabhan, J. Phys. Appl. Phys. 36 (2003) p.990.
- [21] S.D. George, R. Komban, K.G.K. Warriar, P. Radhakrishnan, V.P.N. Nampoouri and C.P.G. Vallabhan, Int. J. Thermophys. 28 (2007) p.123.
- [22] L. Braginsky, V. Shklover, H. Hofmann and P. Bowen, Phys. Rev. B 70 (2004) p.134201.
- [23] E.J. Gonzalez, G. White and L. Wei, J. Mater. Res. 15 (2000) p.744.
- [24] W.M. Lima, V. Biondo, W.R. Weinand, E.S. Nogueira, A.N. Medina, M.L. Baesso and A.C. Bento, J. Phys. Condens. Matter 17 (2005) p.1239.
- [25] D. Jia, D.K. Kim and W.M. Kriven, J. Am. Ceram. Soc. 90 (2007) p.1760.
- [26] S.D. George, A.A. Anappara, K.G.K. Warriar, P. Radhakrishnan, V.P.N. Nampoouri and C.P.G. Vallabhan, Mater. Chem. Phys. 111 (2008) p.38.
- [27] S.D. George, S. Augustine, E. Mathai, P. Radhakrishnan, V.P.N. Nampoouri and C.P.G. Vallabhan, Phys. Status Solidi (a) 196 (2003) p.384.
- [28] S. Fayette, D.S. Smith, A. Smith and C. Martin, J. Eur. Ceram. Soc. 20 (2000) p.297.
- [29] H. Szelagowski, I. Arvanitidis and S. Seetharaman, J. Appl. Phys. 85 (1999) p.193.
- [30] K. Watari, K. Ishizaki and F. Tsuchiya, J. Mater. Sci. 28 (1993) p.3709.
- [31] B. Nait-Ali, K. Haberko, H. Vesteghem, J. Absi and D.S. Smith, J. Eur. Ceram. Soc. 26 (2006) p.3657.
- [32] Z.Y. Deng, J.M.F. Ferreira, Y. Tanaka and Y. Isoda, Acta Mater. 55 (2007) p.3663.
- [33] L. Berginsky, V. Shklover, G. Witz and H.P. Bossmann, Phys. Rev. B (2007) p.94301.
- [34] E. Litoysky, T. Gambaryan-Roisman, M. Shapiro and A. Shavit, *Trends in Heat, Mass and Momentum Transfer*, Vol. 3, Council of Scientific Research Integration, Trivandrum, India, 1997, p.147.
- [35] J.F. Kerrisk, J. Appl. Phys. 42 (1971) p.267.
- [36] H.W. Codbee and W.T. Ziegler, J. Appl. Phys. 37 (1966) p.56.
- [37] D.M. Liu, C.J. Chen and L.J. Lin, J. Appl. Phys. 75 (1994) p.3765.
- [38] A. Sanchez-Lavega, A. Salazar, A. Ocariz, L. Pottier, E. Gomez, L.M. Villar and E. Macho, Appl. Phys. A 65 (1997) p.15, and references therein.
- [39] Z. Zhong and W. Wang, J. Appl. Phys. 100 (2006) p.44310.
- [40] R.W. Rice, J. Mater. Sci. 31 (1996) p.102.
- [41] K. Watari, H. Nakano, K. Sato, K. Urabe, K. Ishisaki, S. Cao and K. Mori, J. Am. Ceram. Soc. 86 (2003) p.1812.
- [42] M.V. Swain, L.F. Johnson, R. Syed and D.P.H. Haseelman, J. Mater. Sci. Lett. 5 (1998) p.799.